Diode-pumped Yb:SSO chirped pulse amplifier with 1 ps pulse duration

Jinfeng Li (李进峰)[1], Peng Gao (高 鹏)[1], Lihe Zheng (郑丽和)[2], Liangbi Su (苏良碧)[2], Jun Xu (徐 军)[2], and Xiaoyan Liang (梁晓燕)[1,3*]

[1]*Shanghai Institute of Optics and Fine Mechanics, Chinese Academy of Sciences, Shanghai 201800, China*

[2]*Shanghai Institute of Ceramics, Chinese Academy of Sciences, Shanghai 2000500, China*

[3]*School of Physical Science and Technology, Shanghai Tech University, Shanghai 200031, China*

[*]*Corresponding author: liangxy@mail.siom.ac.cn*

Received September 1, 2014; accepted December 5, 2014; posted online January 4, 2015

We demonstrate a diode-pumped picosecond Yb-doped silicate Yb^{3+}:Sc_2SiO_5 (Yb:SSO) chirped pulse amplifier. The seed source with a pulse width of 220 fs is a diode-pumped Yb:KGW femtosecond oscillator. A single chirped volume Bragg grating is employed both as a pulse stretcher and as a compressor to improve the compactness of the system. Stretched pulse is amplified using a diode-pumped Yb:SSO regenerative amplifier. The maximum amplified pulse energy obtained at a pump power of 13.5 W is 450 μJ. The amplified pulse is centered at 1033.3 nm before compression at a frequency of 1 kHz. After compression, the pulse energy is 315 μJ with a pulse duration of approximately 1 ps.

OCIS codes: 140. 3580, 140.3280, 140.3615, 140.4050.

doi: 10.3788/COL201513.011403.

In recent years, the high-power, high-energy, and high-repetition rate sub-picosecond to picosecond laser systems have provided possibilities in numerous industrial, medical, and scientific applications, such as high precision micro- and nano-material processing, photo-polymerization, microsurgery, time-resolved spectroscopy, pump/probe analysis, and optical parametric amplification pumping[1–6]. However, these applications require laser systems that are more flexible, robust, reliable, efficient, and compact. According to this background, ultrafast laser systems based on Yb-doped gain media have made a dramatic progress in the most recent period.

Yb-doped media[7] possess several advantageous laser properties, such as low intrinsic quantum defect, absence of up-conversion, excited state absorption, cross-relaxation, and concentration quenching. These properties make Yb-doped media suitable for the development of high-power ultrafast lasers. In recent years, the focus on laser investigations has gradually shifted from oscillators to amplified systems which are able to obtain high-power or high-energy output. Accordingly, various significant results have been reported. In 2010, Russbueldt *et al.*[8] reported a diode-pumped 1.1 kW Yb:YAG Innoslab femtosecond amplifier, which improved the output power of amplifiers based on the Yb-doped gain media to a high level. In 2011, João *et al.*[9] reported a 10 mJ level Yb:KYW diode-pumped regenerative amplifier operating at 10 Hz. Because of its stable performance, this regenerative amplifier was used in the front end of the PHELIX petawatt laser systems at GSI Helmholtz Center. In 2013, Negel *et al.*[10] reported a Yb:YAG thin-disc multi-pass amplifier that delivered ps pulses at an average output power of >1 kW and a pulse energy of >1 mJ. Teisset *et al.*[11] reported a 300 W Yb:YAG thin-disc regenerative amplifier at 10 kHz repetition rate, which delivered pulse energy of 30 mJ. Delaigue *et al.*[12] reported a Yb-doped laser amplifier that can generate a pulse duration of 106 fs and a pulse energy in the order of 100 μJ, which set a new record of pulse width in similar amplifiers. All these inspiring results made us expect that the investigation on Yb-doped laser amplifiers would continue both in terms of gain media and in terms of amplifier architecture.

A newly Yb-doped silicate Yb^{3+}:Sc_2SiO_5 (Yb:SSO) has gained considerable attention in recent years because of its excellent crystalline features, such as broad gain bandwidth (54 nm), high emission cross sections (7.4×10^{-21} cm^2), and good thermal conductivity (7.5 $Wm^{-1}K^{-1}$)[13]. These features indicate the potential use of Yb:SSO in the development of ultrafast, high average power continuous wave (CW), and CW mode-locked (CWML) lasers. Since its first CW operation reported in 2008[13] and CWML operation demonstrated in 2010[14,15], a number of studies have been reported on Yb:SSO oscillators over the last 2 years[16–22]. Nevertheless, its capability for energetic amplification has not been investigated.

In the chirped pulse amplification (CPA) technique, the elements for dispersion compensation commonly include reflecting grating pairs and fibers. However, compared with these components, efforts on exploring elements with more compactness, easier alignment, and higher efficiency have always been made. Several alternative approaches have been explored, such as chirped volume Bragg gratings (CVBGs)[23], linearly chirped fiber gratings[24], linearly chirped quasi-phase

matching structures[25], and hollow-core photonic crystal fiber pulse compressors[26]. Among these approaches, the CVBG, which is written in photo-thermal refractive glass, has been receiving increasing interest. CVBG has several attractive advantages, such as capability of being manufactured in large transverse apertures and ability of handling high pulse energies.

In this letter, we demonstrate a diode-pumped subpicosecond Yb:SSO chirped pulse amplifier. A diode-pumped Yb:KGW femtosecond oscillator is used as a seed source with a pulse width of 220 fs. A single CVBG is employed both as a pulse stretcher and as a compressor to improve the compactness of the system. The stretched pulse is amplified using a diode-pumped Yb:SSO regenerative amplifier. The maximum amplified pulse energy at a pump power of 13.5 W is 450 μJ. The amplified pulse is centered at 1033.3 nm before compression at 1 kHz frequency. After compression, the pulse energy is 315 μJ with a pulse duration of approximately 1 ps. These results confirm that Yb:SSO is a potential material for developing diode-pumped CPA lasers.

The experimental setup is shown in Fig. 1. A homemade oscillator based on Yb:KGW crystal is used as seed source. The oscillator delivers pulses centered at 1035 nm with a spectral full-width at half-maximum (FWHM) bandwidth of 8 nm at a repetition rate of 53 MHz. The pulse width is 220 fs and the average power is 260 mW. A single CVBG (OptiGrate Corp.) is used both as a stretcher and as a compressor in the CPA scheme. This method enables a more compact and robust stretcher–compressor system than the conventional diffraction gratings, which are normally wide and require time-consuming alignment[27]. The CVBG used in this experiment has a square aperture of 5×5 (mm) and a length of 32 mm. The central wavelength of the CVBG is 1040±2 nm with a spectral bandwidth of 25±2 nm. The grating reflection efficiency is approximately 70%. Eventually, the stretched pulse width is measured to be approximately 50 ps.

A pockels cell (PC1, Fastpulse Technology Inc.) is used as a pulse picker to pick the injected pulse from the oscillator. The electro-optic crystal of the PC is BBO, which has a clear aperture of 4 mm in diameter. The length of the BBO is 25 mm. Its half-wave and quarter-wave voltages are 7.8 and 3.9 kV, respectively. The beam radius on the BBO is approximately 1 mm. The maximum operating frequency of the PC is 5 kHz. And in the experiment, the operating frequency is chosen to be 1 kHz. Because the polarization of the seed pulse is parallel to the baseplate, a $\lambda/2$ wave plate is used to alter the polarization of the picked pulse. An isolator, composed of a Faraday rotator, a $\lambda/2$ wave plate, and a thin film polarizer (TFP1), is employed to separate the amplified pulses from the counterpropagating injected seed pulses. The amplified pulses are reflected out from the TFP1.

A classic folded resonator is used as amplifier cavity. A 30 W fiber-coupled diode laser is employed as pump source, which has a core-diameter of 200 μm and numerical aperture of 0.22, emitting at the wavelength of 976 nm at room temperature. A series of lenses, which have an image ratio of 1:1, are used to focus the pump beam into the crystal. The cavity is designed to provide a mode size diameter of 220 μm inside the crystal. The 5 at.% Yb:SSO crystal (5 × 6 × 3 (mm)), which is coated for antireflection (AR) at lasing and pump wavelengths on both faces, is wrapped with indium foil and mounts in a water-cooled copper block. The absorption of pump power of the crystal is measured to be 70%. The water temperature is maintained at 15 °C. A PC2, which has the same parameters as PC1, is used to switch out the amplified pulses. The amplified beam radius in the PC2 is designed to be 0.8 mm. The total length of the cavity is 1.88 m. All elements of the amplifier cavity fit inside a 120 × 50 (cm) footprint.

In the amplification stage, the PC2 is precisely synchronized with PC1 through external control circuits. The gate voltage of PC2 is applied when the seed pulse is just reflected from highly reflective (HR) mirror and passed through PC2; hence, the delay between PC1 and PC2 is set to be 5 ns.

A maximum amplification output power of 450 mW is obtained at a pump power of 13.5 W when the gate width of PC2 is set to be 800 ns (corresponding to 64 roundtrips). The corresponding single pulse energy is 450 μJ. Figure 2 illustrates the dependence of the laser output power versus incident pump power during amplification. Increasing the pump power would lead to saturation of the output power. And furthermore,

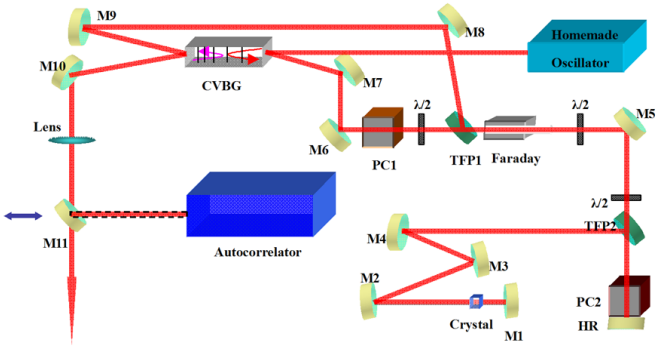

Fig. 1. Schematic of Yb:SSO CPA system.

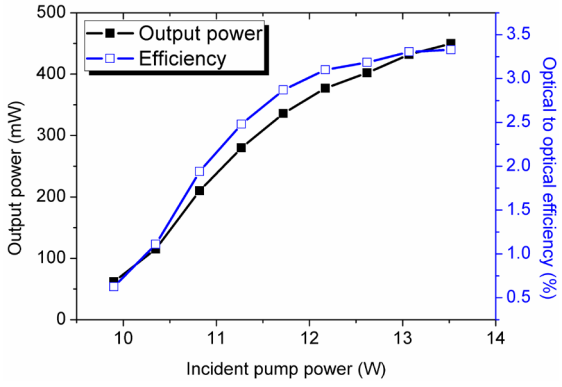

Fig. 2. Dependence of laser output power on absorbed pump power in amplification process.

increasing pump power could even damage the AR coating of the crystal. This phenomenon, which is caused by the over high power density, is due to a small beam size and a relatively narrow duration of the amplified pulse in the crystal. Thus, in future experiments, in order to obtain higher amplified output power, the mode size in the amplified crystal should be expanded, and the seed pulse should be stretched even further to a broader pulse width.

After amplification, the pulse is extracted through TFP1 and passes through the same CVBG, but in opposite direction of the pulse compression. In order to obtain higher reflection efficiency from CVBG, the incident angle is maintained as minimal as possible. The single pulse energy is 315 μJ after compression, corresponding to a reflection efficiency of 70%. Compared with the efficiency of linearly chirped fiber grating (80%)[24] and hollow-core photonic crystal fiber (73%)[26], the grating efficiency of CVBG is not relatively high. It is limited by the incident angle of the beam. Decreasing the incident angle would lead to a higher grating efficiency. However, the actual angle of incidence is restricted by the spatial layout of the system.

A FX-103L autocorrelator (Femtochrome Inc.) is used to measure the pulse duration. The minimum pulse width obtained is 1.3 ps, assuming the pulses have a Gaussian-shaped temporal intensity profile. The pulse autocorrelation trace is shown in Fig. 3. A HR4000 fiber spectrometer (Ocean Optics Inc.) is used to measure the spectra of the pulse. The spectra of the seed and the amplified pulses are shown in Fig. 4. The central wavelength of the amplified pulse is 1033.3 nm with a FWHM width of 2.5 nm. The time-bandwidth product is calculated to be 0.84. This result indicates that an excess chirp is generated during the amplification process because the pulse passes the crystal many times. In this experiment, stretch and compression of the pulses are accomplished using the same CVBG. It can only compensate for its own dispersion, but could not compensate the second- and third-order dispersions that are caused by the gain medium. In order to obtain shorter pulse width, the HR mirror in the amplification cavity is replaced by a Gires-Tournois interferometer (GTI) mirror that can provide –2000 fs^2 dispersion compensation at a single reflection.

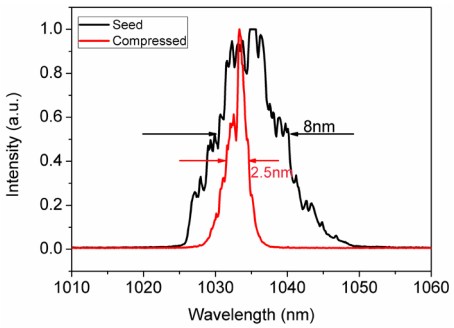

Fig. 4. Spectral profile of seed and compressed amplified pulse.

The shortest pulse width achieved is 1.06 ps, and the autocorrelation trace is also shown in Fig. 3.

As can be seen from Fig. 4, the spectral width of the amplified pulse is narrowed to a certain extent, which is caused by the gain narrowing effect, compared with that of the seed pulse spectra. Subsequently, this phenomenon increased the achievable pulse width. Hence, in future experiments, some counteracting gain narrowing techniques, such as spectral amplitude shaping, should be applied to generate shorter pulse duration.

Figure 5 illustrates the M^2 factor of the amplified pulse, which is measured when the output power is 200 mW after compression. The result is close to the diffraction limit, giving a beam quality of M^2_x = 1.25 and M^2_y = 1.18 in both directions perpendicular to the axis of propagation. A beam profile of the amplified pulse is also measured in the position where the beam is reflected from CVBG in the compression process with a charge-coupled device camera and is shown in the inset of Fig. 5, indicating a TEM_{00} mode. These beam quality results demonstrate no obvious change with pump power.

In conclusion, we demonstrate a diode-pumped sub-picosecond Yb:SSO chirped pulse amplifier. The maximum amplified pulse energy obtained at a pump power of 13.5 W is 450 μJ. The amplified pulse is centered at 1033.3 nm before compression at a frequency of 1 kHz. After compression, the pulse energy is 315 μJ with a pulse duration of approximately 1 ps. The efficiency of the amplification is relatively low, which may be due to the slightly high insertion loss in the cavity. Therefore, in

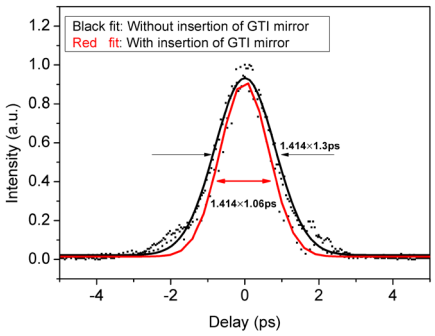

Fig. 3. Autocorrelation trace without and with GTI inserted in amplifying cavity.

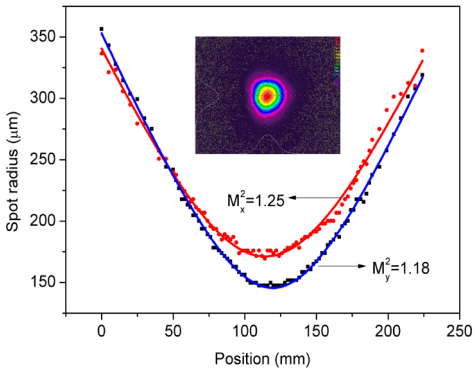

Fig. 5. M^2 factors for both directions perpendicular to the axis of propagation.

the following experiment, the insertion loss of the cavity needs to be well controlled to improve the efficiency. It can also be anticipated that, in further experiment, pulses with high energy and short duration can be obtained through enlargement of beam size inside the crystal and by using spectral amplitude shaping to suppress the gain narrowing effect. This work confirms that Yb:SSO has a high potential for developing diode-pumped CPA lasers. Regenerative amplifiers based on this material canhave important application in areas such as micro-machining, biological imaging, and nonlinear spectroscopy.

This work was supported by the National Science Foundation of China under Grant No. 61378030.

References

1. J. Kleinbauer, R. Knappe, and R. Wallenstein, Appl. Phys. B **80,** 315 (2005).
2. M. Malinauskas, A. Zukauskas, G. Bickauskaite, R. Gadonas, and S. Juodkazis, Opt. Express **18,** 10209 (2010).
3. L. H. Christopher, N. J. Durr, P. Chen, W. Piyawattanametha, H. Ra, O. Solgaard, and A. Ben-Yakar, Opt. Express **16,** 9996 (2008).
4. A. Bartels, T. Dekorsy, and H. Kurz, Opt. Lett. **24,** 996 (1999).
5. P. Wu, C. Sui, and W. Huang, Photon. Res. **2,** 82 (2014).
6. X. Ni, K. K. Anoop, M. Bianco, S. Amoruso, X. Wang, T. Li, M. Hu, and Z. Song, Chin. Opt. Lett.**11,** 093201 (2013).
7. F. Druon, F. Balembois, and P. Georges, C. R. Phys. **8,** 153 (2007).
8. P. Russbueldt, T. Mans, J. Weitenberg, H. D. Hoffmann, and R. Poprawe, Opt. Lett. **35,** 4169 (2010).
9. C. P. João, J. Körner, M. Kahle, H. Liebetrau, R. Seifert, M. Lenski, S. Pastrik, J. Hein, T. Gottschall, J. Limpert, and V. Bagnoud, Proc. SPIE **8080,** 808008 (2011).
10. J. P. Negel, A. Voss, M. A. Ahmed, D. Bauer, D. Sutter, A. Killi, and T. Graf, Opt. Lett. **38,** 5442 (2013).
11. C. Y. Teisset, M. Schultze, R. Bessing, M. Häfner, S. Prinz, D. Sutter, and T. Metzger, in *Proceedings of Advanced Solid-State Lasers Congress* JTh5A (2013).
12. M. Delaigue, J. Pouysegur, S. Ricaud, C. Hönninger, and E. Mottay, Proc. SPIE **8611,** 86110J (2013).
13. L. Zheng, J. Xu, G. Zhao, L. Su, F. Wu, and X. Liang, Appl. Phys. B **91,** 443 (2008).
14. W. D. Tan, D. Tang, X. Xu, J. Zhang, C. Xu, F. Xu, L. Zheng, L. Su, and J. Xu, Opt. Express **18,** 16739 (2010).
15. J. Li, X. Liang, J. He, L. Zheng, Z. Zhao, and J. Xu, Opt. Express **18,** 18354 (2010).
16. K. S. Wentsch, L. H. Zheng, J. Xu, M. A. Ahmed, and T. Graf, Opt. Lett. **37,** 4750 (2012).
17. L. M. Su, J. Liu, C. Feng, X. W. Fan, L. H. Zheng, L. B. Su, and J. Xu, Laser Phys. **22,** 503 (2012).
18. L. M. Su, Y. G. Wang, J. Liu, L. H. Zheng, L. B. Su, and J. Xu, Laser Phys. Lett. **9,** 120 (2012).
19. C. Liu, Y. Wang, J. Liu, L. Zheng, L. Su, and J. Xu, Opt. Commun. **285,** 1352 (2012).
20. W. D. Tan, D. Tang, X. Xu, J. Zhang, C. Xu, F. Xu, L. Zheng, L. Su, and J. Xu, in *Proceedings of Photonics Global Conference* (2010).
21. C. Xu, D. Tang, J. Zhang, H. Zhu, X. Xu, L. Zheng, L. Su, and J. Xu, Opt. Commun. **294,** 237 (2013).
22. H. Zhang, J. Li, X. Liang, H. Lin, L. Zheng, L. Su, and J. Xu, Chin. Opt. Lett. **10,** 111404 (2012).
23. K. Liao, M. Cheng, E. Flecher, V. I. Smirnov, L. B. Glebov, and A. Galvanauskas, Opt. Express **15,** 4876 (2007).
24. A. Galvanauskas, M. E. Fermann, D. Harter, K. Sugden, and I. Bennion, Appl. Phys. Lett. **66,** 1053 (1995).
25. A. Galvanauskas, M. A. Arbore, M. M. Feijer, and D. Harter, Opt. Lett. **23,** 1695 (1998).
26. J. Limpert, T. Schreiber, S. Nolte, H. Zellmer, and A. Tuennerman, Opt. Express **11,** 3332 (2003).
27. C. P. João, J. Körner, M. Kahle, H. Liebetrau, R. Seifert, M. Lenski, S. Pastrik, J. Hein, T. Gottschall, J. Limpert, G. Figueira, and V. Bagnoud, Proc. SPIE **8001,** 80011E (2011).